Neuropsychopharmacology (2006) 31, 572–584

www.neuropsychopharmacology.org

NrCAM in Addiction Vulnerability: Positional Cloning, Drug-Regulation, Haplotype-Specific Expression, and Altered Drug Reward in Knockout Mice

Hiroki Ishiguro[1], Qing-Rong Liu[1], Jian-Ping Gong[1], Frank Scott Hall[1], Hiroshi Ujike[2], Marisela Morales[3], Takeshi Sakurai[4], Martin Grumet[5] and George R Uhl*[,1,3]

[1]Molecular Neurobiology Branch, NIDA-IRP, NIH, Baltimore, MD, USA; [2]Department of Neuropsychiatry, Okayama University Medical School, Okayama, Japan; [3]Cellular Neuroscience Branch, NIDA-IRP, Baltimore, MD, USA; [4]Department of Neurobiology, Mt Sinai School of Medicine, New York, NY, USA; [5]Keck Ctr Collab. Neurosci, Rutgers University, Piscataway, NJ, USA

Several lines of evidence support roles for the cell adhesion molecule *NrCAM* in addictions. Fine mapping within a chromosome 7 region that contains previously linked and associated genomic markers identifies *NrCAM* haplotypes that are associated with substance abuse vulnerabilities in four samples of abusers and controls. Differential display identifies *NrCAM* as a drug regulated gene. *NrCAM* is expressed in neurons linked to reward and memory. *NrCAM* displays haplotype-specific gene expression in human post-mortem brain samples. Knockout mice display reduced opiate- and stimulant-conditioned place preferences. These observations support *NrCAM* as a positionally cloned and drug-regulated gene whose variants are likely to change expression and alter substance abuse vulnerabilities in human addictions and animal models of drug reward.

Neuropsychopharmacology (2006) **31,** 572–584. doi:10.1038/sj.npp.1300855; published online 10 August 2005

Keywords: neuronal adhesion; gene regulation; addiction; association; morphine

INTRODUCTION

Molecular biology and molecular genetics provide complementary approaches to the interesting but complex problems posed by human addictions. There are large complex genetic influences on human substance abuse vulnerabilities (Kendler *et al*, 1994, 1999, 2000; Gynther *et al*, 1995; Tsuang *et al*, 1996, 1998, 1999; Uhl *et al*, 1997; Kendler and Prescott, 1998; Merikangas *et al*, 1998; Stallings *et al*, 1999; True *et al*, 1999a, b; Uhl, 1999, 2004; Karkowski *et al*, 2000). Much of the genetic vulnerability to abuse of different legal and illegal addictive substances is shared. Linkage- and association-based genome scanning studies have identified a number of chromosomal regions likely to contain variants that confer vulnerabilities to dependence on illegal substances, ethanol and/or nicotine (Uhl *et al*, 2002; Uhl, 2004). The mid region of human chromosome 7 is an interesting candidate site for allelic variants that alter substance abuse vulnerability based on linkages to alcoholism and associations with polysubstance abuse (Reich, 1996; Long *et al*, 1998; Reich *et al*, 1998; Uhl *et al*, 2001, 2002).

Molecular biologic studies of drug-induced gene regulation provide another approach to understanding substance abuse. We and others have used differential display and microarray approaches to identify constellations of gene expression patterns that are altered by acute or chronic administration of morphine and other addictive substances (Douglas *et al*, 1995; Wang *et al*, 1997; Schafer *et al*, 2001; Toyooka *et al*, 2002; Savoie *et al*, 2003; Sokolov *et al*, 2003). Identifying convergent data from genome scanning studies and studies of gene regulation could help to focus on interesting aspects of the large data sets generated by each of these approaches.

We now report results of association-based fine mapping of the chromosome 7 regions that contains positive markers from prior linkage and association studies, WIAF1680, D7S1793, D7S1830, and D7S1809. We describe initial identification of *NrCAM* based on convergence between initial association findings in this region and results from studies of morphine-regulated gene expression. We report additional fine mapping results that provide *NrCAM* haplotypes that are associated with substance abuse vulnerability in several samples and with different levels of *NrCAM* mRNA expression in human post-mortem tissue samples. We document reduced reward from morphine,

*Correspondence: Dr GR Uhl, Molecular Neurobiology Branch, NIDA-IRP, NIH, Box 5180, Baltimore, MD 21224, USA, Tel: +1 410 550 2843 ext. 146, Fax: +1 410 550 1535, E-mail: guhl@intra.nida.nih.gov
Received 24 February 2005; revised 26 April 2005; accepted 3 June 2005
Online publication: 30 June 2005 at http://www.acnp.org/citations/Npp0630050050127/default.pdf

cocaine, and amphetamine, which is manifest in mice with reduced *NrCAM* expression. This converging evidence supports involvement of *NrCAM* and its regulation in mechanisms of reward and in addiction vulnerability. This converging evidence also supports contributions of common *NrCAM* allelic variants to human individual differences in addiction vulnerability.

MATERIALS AND METHODS

Subtracted Differential Display, Northern, and RT-PCR Experiments

Male Sprague–Dawley rats (250–300 g) and male wild-type C57/BJ mice (25–30 g) were housed under 12-h light/12-h dark conditions and given food and water *ad libitum*. Morphine treatments for rat subtracted differential display experiments were 20 mg/kg morphine or saline i.p. with killing 4 h after injection. For RT-PCR experiments, mice were treated with saline or with 20 or 100 mg/kg/i.p. morphine and killed 4 h after the last injection.

Brains were rapidly removed, regions dissected, and total and polyA$^+$ RNAs were extracted. Subtracted differential display was performed as described (Wang *et al*, 1997), with sequence comparisons using BLAST (National Library of Medicine, Bethesda, MD). Northern analyses were carried out as described (Liu *et al*, 2002). RT-PCR experiments used *TaqMan* real-time PCR expression assays, an ABI 7900HT Sequence Detection System and *TaqMan* GAPDH control reagents (ABI, Foster City, CA, USA). *NrCAM* mRNA was assessed using oligonucleotide primers 5′-AGTGATGCA GAAGATC and 5′-GATGATGGGACGTTTGGAGAATAC and probe 5′-TCCTGTCT GAAGGTGTTCGACTT.

Identification of *NrCAM* cDNAs

Plaques (8×10^6) from a size-selected rat brain DNA library prepared in lambda ZAP II (Stratagene, La Jolla, CA) were screened using a 340 bp *Eco*RI fragment of the MD50 product radiolabeled by random priming with (^{32}P)dCTP as described (Liu *et al*, 1993). DNAs from 17 positively hybridizing plaques obtained from three cycles of plaque purification were sequenced using dideoxynucleotide termination manual and automated methods. These sequences were assembled into 6783 and 7099 bp subclones termed NC1–4 subclone and NC2–5, respectively.

Human *NrCAM* Sequences and Variants and their Homology with Mouse and Rat Sequences and Variants

Human N*rCAM* sequences came from NCBI (http://www.ncbi.nlm.nih.gov) and Celera databases (http://www.celeradiscoverysystem.com/index.cfm). Human genomic and cDNA sequences included BAC and scaffold sequences AC005058, AC007567, AC005683, AF172277, hCG17111, hCG1654651, hCG1654652, hCG1806278, and GA_x54KREB-2RL0. We assembled more than 400 kb of human *NrCAM* genomic sequence, with attention to correcting scrambled and/or misaligned sequences found in the original sources. Human sequences were also compared to mouse and rat cDNA and genomic sequences from NCBI and Celera databases that included mCT6280, mCT6282, mCG7335, mCG7337, GAx5J8B7TUNR9, GAx5J8B7W4G5V, and NW_047760. Variants were sought by assembly of sequences obtained from DNAs of different individuals and by resequencing amplicons obtained from DNA from different individuals. Haplotypes were sought in BAC sequence comparisons, with attention to comparisons between AC005683 sequences and those forming a consensus from other assembled sequences.

Human Subjects for Association Genome Scanning

DNAs came from NIDA research volunteers of self-reported European- and African-American descent balanced for gender whose drug use and dependence were characterized as described (Smith *et al*, 1992; Persico *et al*, 1996; Uhl *et al*, 2001). Unrelated European-American 'abusers' averaged 35 years of age, scored the maximal 3+ score on a total drug use scale of use of addictive substances, and/or demonstrated DSMIII-R or DSMIV dependence on at least one illegal abused substance. 'Control' European-Americans averaged age 32 reported no significant lifetime histories of use of any addictive substance and 0 or 1+ DUS total drug use scores indicating that this group mixed individuals with little or no lifetime experience with legal or illegal addictive substances. 'Abusers' of self-reported African-American descent averaged 34 years of age while 181 controls averaged 36 years of age. We excluded subjects with 2+ DUS scores who did not reach DSM dependence criteria for an illegal substance. Other DNAs came from 177 unrelated individuals selected from COGA (wave I) pedigrees generously supplied from NIAAA with the assistance of COGA investigators. The substance abusing proband was selected from each pedigree based on (a) diagnosis of alcohol dependence and (b) manifestation of the highest level of abuse or dependence on illegal substances of any individual within that pedigree. Controls with no histories of substance abuse or dependence were selected from individuals who married into these pedigrees. A fourth sample contains 288 alcohol-dependent Japanese subjects and 472 gender-balanced Japanese control research volunteers who reported no alcoholism or dependence on other illegal substances, as previously described (Ishiguro *et al*, 1998). Alcohol-dependent individuals averaged 52 years of age when tested and 37 years of age at the onset of their alcohol dependence. Controls averaged 49 years of age were selected from healthy volunteers, who displayed no psychiatric diagnoses and reported levels of alcohol use less than two drinks on fewer than two occasions per week during any year.

Genotyping

Alleles for 54 SNPs lying in the mid chromosome 7 region of interest were assessed in DNA pools using SNP microarrays as described (Uhl *et al*, 2001). Alleles of 37 additional simple sequence length polymorphism (SSLP) markers were assessed in pooled DNA samples based on peak heights in ABI 3100 chromatograms. A total of 11 SNPs were genotyped by PCR-restriction fragment length polymorphism (RFLP) methods using 3% agarose/1.5% NuSieve gels, ethidium bromide staining, and ultraviolet transillumination. Additional SNPs at the *NrCAM* locus were genotyped

with 5′ nuclease assays using TaqMan/ABI 7900HT sequence detection system assays and SnapShot/ABI 3100 genetic analyzer assays. Nominal significance values are reported for results from samples that nominated regions for further analyses. Significance values are reported for hypothesis-directed studies that replicate associations at these markers. Nominal significance values are reported for associations using haplotypes generated in studies of mRNA expression in brains of heterozygous individuals (see below).

Allele-Specific Expression in Human Brain RNAs

Brains were surgically removed from epileptic patients and/or obtained post mortem (Brain Tissue Bank at University of Maryland). Samples heterozygous for selected *NrCAM* markers were identified. Total and polyA$^+$ RNAs and cDNAs were prepared from these specimens as described above. Allele-specific expression was assessed using: (a) real-time PCR, SNP-specific genotyping primers and probes and an ABI7900HT sequence detection system or (b) cDNAs amplified by PCR so that the allele-specific primer extension products produced peaks whose heights could be determined using an ABI 3100 (SnapShot, ABI, Foster City, CA) analyzer, compared to results obtained from genomic DNAs and normalized by comparison to standards constructed using known samples mixed in differing proportions. To specify the haplotypes conferring differential expression, we focused on alleles whose cDNA expression differences were larger than twice the standard deviation of the techniques used, as assessed in data from heterozygote genomic DNAs studied in parallel with the cDNA samples.

In Situ Hybridization and Immunohistochemistry

Adult rats and C57BL/6 mice were anesthetized, perfused, brains dissected, postfixed, equilibrated, and cut at 20–40 μm as described (Moriwaki *et al*, 1996). *In situ* hybridization (Uhl and Kitayama, 1993; Morales and Bloom, 1997) used (a) antisense T3 and control sense T7 transcripts that corresponded to the 0.2 kb 3′-UTR of clone NC9 sequences radiolabelled with [^{35}S]UTP and (b) a 45 base antisense oligonucleotide complementary to *NrCAM* 3′-untranslated region sequences AACGAAGTACCC AACCAC GTCGCA ATCACATACACAG CTAGTCCT that was internally radio-labeled with [^{35}S]dCTP. Immunofluoresence (McNaught *et al*, 2002) used goat anti-*NrCAM* (Santa Cruz), rabbit antidopamine transporter (Chemicon), Alexa fluor 594 (red) anti-goat and Alexa fluor 488 (green) anti-rabbit secondary antibodies (Molecular Probes), and confocal microscopy.

Morphine- and Cocaine-Conditioned Place Preference

NrCAM knockout mice (25–30 g) were produced as described, maintained on mixed C57/129 genetic backgrounds under conditions noted above, and bred by heterozygote-heterozygote breeding strategies so that the average genetic backgrounds of homozygous *NrCAM* knockout, heterozygous *NrCAM* knockout, and matching wild-type mice were identical (Sakurai *et al*, 1997). Neither homozygous nor heterozygous *NrCAM* knockout mice displayed abnormal body size, locomotor activity, or growth rates, as previously noted (Sakurai *et al*, 1997). Conditioned place preferences were assessed as described (Sora *et al*, 2001). There were 4-day conditioning sessions using morphine sulfate (20 mg/kg i.p.; 30 min exposures), cocaine (20 mg/kg s.c; 20 min exposures), or amphetamine (2.0 mg/kg i.p.; 20 min exposures) with horizontal locomotor activity monitored during these trials as described (Hall *et al*, 2004). Conditioned place preference was calculated as the difference in the duration of time spent in the drug-paired compartment before and after drug conditioning. A positive score thus represents a preference for the drug-paired environment.

Statistical Analyses

Genotype frequencies were fit to Hardy–Weinberg equilibrium values, maximum-likelihood haplotype frequencies were estimated using expectation-maximization (EM) algorithms and Arlequin ver 1.1 (http://lgb.unige.ch/arlequin/) and standardized linkage disequilibrium estimates ($D' = D/D_{max}$) were computed from estimated haplotype frequencies. For SSLP genotyping with pooled DNA analysis, estimated frequencies of each allele were multiplied by the total number of alleles in each pool. Differences in observed allele, genotype frequencies, and haplotype frequencies between groups were tested for nominal significance using Fisher's exact tests on 2×2 or $2 \times$ (number of genotypes) contingency tables. For comparisons of initial screening estimates of allele and haplotype frequencies, p-values < 0.05 were considered nominally significant. Nominally significant results from initial association studies were then tested in additional samples. Behavioral results were assessed using one-way ANOVA and *post hoc* t-tests. RNA expression data were assessed using t-tests.

RESULTS

Identification of *NrCAM* as a Morphine-Regulated Gene

Subtracted differential display results. Subtracted differential display PCR (SDD) identified MD50 as one of more than 40 regulated subcloned SDD cDNAs that corresponded to mRNAs whose expression was altered in striata of rats killed 4 h after treatment with 20 mg/kg morphine. MD50 displayed a 340 bp sequence with strong nucleotide similarities to human sequences 3860–4134 bp of GenBank entry U55258 previously reported as 3′ untranslated sequences of *NrCAM*.

A radiolabeled 340 bp MD50 fragment identified full-length cDNAs in a rat cerebral cortex λZapII library (Clontech, Palo Alto, CA). Sequences obtained from these clones defined the full-length *NrCAM* cDNA and several apparent *NrCAM* isoforms.

Full-length *NrCAM* cDNAs encode a single-transmembrane-domain protein with an N-terminal signal peptide, six immunoglobulin (Ig) domains, four to five fibronectin III repeats, a transmembrane domain, and a C-terminal cytoplasmic domain with tyrosine kinase phosphoacceptor sites (FIGQY) (Figure 1). Multiple rat *NrCAM* isoforms were also identified as the products of differential RNA splicing

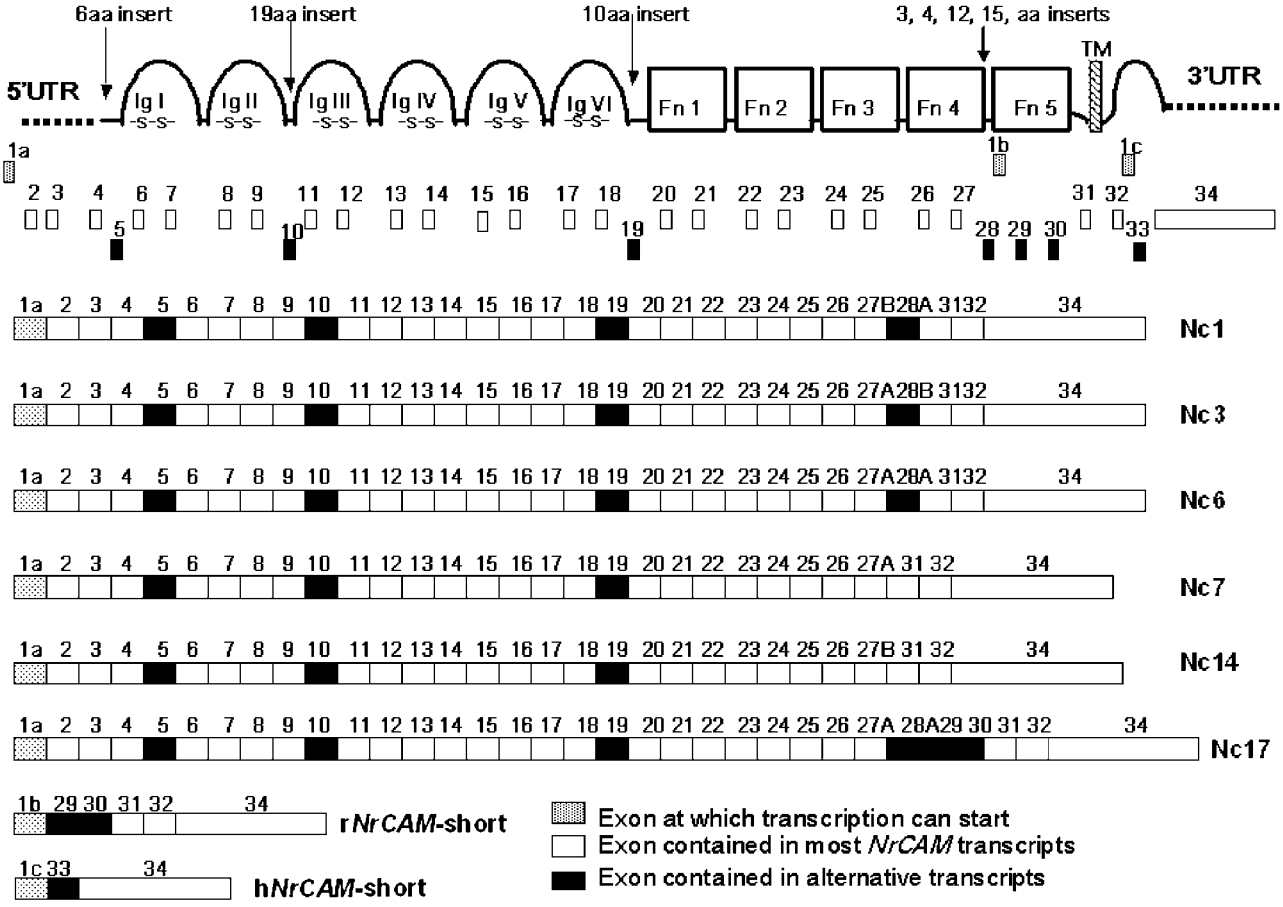

Figure 1 (*Top row*) Cartoon of *NrCAM*'s structure with fibronectin, immunoglobulin, transmembrane, and intracellular (C-terminal) domains indicated. Arrows indicate sites where splice variants encode additional inserted additional amino acids. These *NrCAM* structures are conserved in human, mouse, and rat. (*Second row*) Cartoon of the distribution of *NrCAM* exons, including those used in most transcripts (*open boxes*) and those that are alternatively spliced (*filled boxes*). Most exons are conserved in human, mouse and rat. Exons 1b and 33 have not been identified in humans. The candidate alternatively transcribed exons produce the shorter rat and human isoforms are shown in the bottom two rows. (*Rows 3–8*) NrCAM clones (Nc)1, 3, 6, 7, 14, 17 that represent splice variant isoforms identified in rat brain cDNAs. (*Rows 9–10*) Shorter *NrCAM* gene product expressed isoforms that are identified from ESTs in rat and human databases.

that produced *NrCAM* translation products with short inserted peptide sequences (Figure 1).

NrCAM cDNA and Genomic Sequences: Human, Rat, Mouse

Intron/exon structures of NrCAM *genes from several species.* Assembly of human *NrCAM* cDNA and genomic sequences reveals 35 exons encompassing 300 kb of chromosome 7q31.1–31.2. At least a dozen *NrCAM* isoforms can be produced from these exonic sequences by alternative splicing and transcriptional start site usage (Wang *et al*, 1998). Mouse and rat *NrCAM* cDNA and genomic sequences reveal 36 *NrCAM* exons that encompass about 300 kb of mouse chromosome 12A3 and rat chromosome 6q16.

Sequences that flank each *NrCAM* exon contain consensus splicing acceptor (AG) and donor (GT) sites. 5′-untranslated regions (UTRs) of both human and rodent *NrCAM* mRNAs are encoded by exons 1–3. These exons are separated by 60, 70–80, and 70–80 kb introns, respectively. Other *NrCAM* exons lie within 70–90 kb regions of both human and rodent genomic sequences. Most of these *NrCAM* exons encode functional domains. Two exons encode each Ig or fibronectin domain, one exon encodes the signal peptide, one encodes the transmembrane domain, and two encode the intracellular domain and 3′UTR (Figure 1). *NrCAM* exon–intron structures from human, mouse, and rat are well conserved. *NrCAM* peptides from these species share $\geqslant$93% identity.

Alternative NrCAM *promoters, splice variants and isoforms.* Analyses of 17 rat *NrCAM* cDNA clones reveal both novel and previously identified splicing isoforms. The six amino acid insertion encoded by exon 5 is located between the signal peptide and the first Ig domain. The 19 amino acid insertion encoded by exon 10 falls between Ig domains II and III. The 10 amino acid insertion encoded by exon 19 is located between the Ig domain VI and the first fibronectin III (FnIII) domain. The C-terminus of the fourth fibronectin domain displays substantial variability that is conferred by isoforms that include a three amino acid insertion encoded by exon 27B, a 15 amino acid insertion encoded by exons 27B and 28A and 12- and four amino acid insertions encoded by exons 28A and B, respectively. Exons 28, 29, and

30 encode 93 and 105 amino acid insertions that include a fifth fibronectin domain (Figure 1). A novel isoform found in both mouse and rat *NrCAM* genes uses an additional *NrCAM* exon that we term rodent exon 1b. This exon encodes an alternative transcriptional start site that could not be identified in human EST or genomic sequences. Transcription beginning at the 5′ end of rodent exon 1b produces the 4.5 kb mRNA identified in rodent Northern studies (*see below*). This exon's products are also identified in transcripts mCT6282 and AU08595 that contain only *NrCAM*'s fifth fibronectin, transmembrane, and intracellular domains. An additional novel *NrCAM* isoform observed in both human and rodent genomic and EST (BG001715) sequences uses exons 1c, the unique exon 33 and then the common exon 34 to produce an *NrCAM* isoform that contains only the intracellular domain of other *NrCAM* isoforms (Figure 1). Transcription of the human *NrCAM* is thus likely to start at two promoters. Transcription of the rodent *NrCAM* is likely to utilize three promoters to create *NrCAM* isoforms with different structures.

NrCAM Expression and Regulation

Northern and RT-PCR analyses. Northern analyses reveal *NrCAM* mRNA in rat brain but not in spleen, muscle, lung, liver, kidney, or heart (Figure 2). These analyses reveal 7.8, 6.5, 6.0, and 4.5 kb brain mRNA species likely to represent several *NrCAM* alternative splice and transcriptional start site variants. *NrCAM* mRNA displays high expression in cerebral cortex and hippocampus and moderate levels in striatum and thalamus.

Rats killed after single treatments with 20 mg/kg morphine reveal *NrCAM* mRNA upregulation to 183 ± 20, and $141 \pm 10\%$ of control values in Northern analyses of mRNA from striatum, and cortex, respectively. RT-PCR analyses of *NrCAM* expression in brains of wild-type mice killed after the same morphine doses reveal *NrCAM* levels that are 107 ± 4, 110 ± 7, $115 \pm 7\%$ of control values in striatum, midbrain, and hippocampus, respectively.

In situ *hybridization. In situ* hybridization using *NrCAM* cRNA and oligonucleotide cDNA hybridization probes complementary to 3′ untranslated region sequences common to all *NrCAM* isoforms produce largely similar patterns for brain distribution that are not found when mRNA-sense hybridization probe is applied in control experiments (Figure 3) using film and emulsion autoradiography. The majority of hybridization signal is associated with neurons. White matter tracts including the corpus callosum, anterior commissure, and cerebellar peduncles display only background autoradiographic grain densities.

NrCAM mRNA expression is high in hippocampal pyramidal cells. Scattered neurons in other hippocampal layers also display significant hybridization densities. Higher densities of hybridization in mid- to deep layers of the cerebral cortex noted on film autoradiograms correspond to especially high levels of hybridization to the largest neurons in cerebral cortical laminae V and VI. Cerebellar purkinge cells display high densities of hybridization. In the striatum, hybridization densities are highest over large neurons consistent with interneurons. Hypothalamic zones contained spotty hybridization densities, including moderate hybridization signals over neurons of the supraoptic and paraventricular nuclei. Densities are noted in the habenula and basal medulla, including inferior olive and nucleus raphé magnus. Cells of the substantia nigra and ventral tegmental area (VTA) express hybridization densities.

Densities over individual cells in the nucleus paranigralis of the VTA are similar to those of hippocampal pyramidal neurons. *NrCAM* immunoreactivity is also found in ventral midbrain neurons (Figure 3). Many, but not all, of the *NrCAM* immunopositive neurons in the VAT also express dopamine transporter (DAT) immunoreactivity, a marker for dopaminergic neurons (Figure 3g–i). However, minor *NrCAM* immunopositive neuronal subpopulations do not clearly express DAT and minor subgroups of DAT immunopositive neurons fail to clearly express *NrCAM* (*data not shown*).

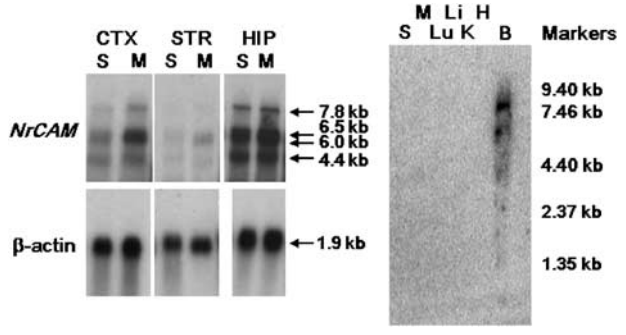

Figure 2 *NrCAM* mRNA size, distribution, and regulation. Northern analyses of *NrCAM* distribution and its regulation by saline (S) and morphine (M) treatment in cortex (CTX), striatum (STR), and hippocampus (HIP). There is substantial expression of several *NrCAM* transcripts in brain (B) but not in heart (H), lung (L), kidney (K), liver (L), skeletal muscle (M), or spleen (S).

Association Genome Scanning of the Chromosome 7 Region of Interest

Hypothesis generation: NrCAM *variants might contribute to individual differences in human addiction vulnerability.* In total, 11 of 37 tested mid-chromosome 7 simple sequence polymorphisms display allele frequency differences between abusers and controls in NIDA European- and/or African-American samples that reach nominal significance (eg uncorrected for multiple comparisons). Three display nominally significant differences in both populations, while fewer than one would have been expected by chance. The nominally significant results thus encompass WIAF1680, D7S2420, and other markers located between 98 and 103 Mb of chromosome 7, a region that contains *NrCAM*. Since we had just identified this gene as drug-regulated, we used these nominally significant results and this expression data to generate the testable hypothesis that allelic variants in *NrCAM* might contribute to individual differences in human addiction vulnerability.

We also tested alternative hypotheses by studying markers in other nearby genes that include intracellular membrane-associated calcium-independent phospholipase A2γ (*iPLA2*)(hCG17116, XM_027224), a ribosomal protein L7 homologue (hCG17114, XM_027229), the laminin-β

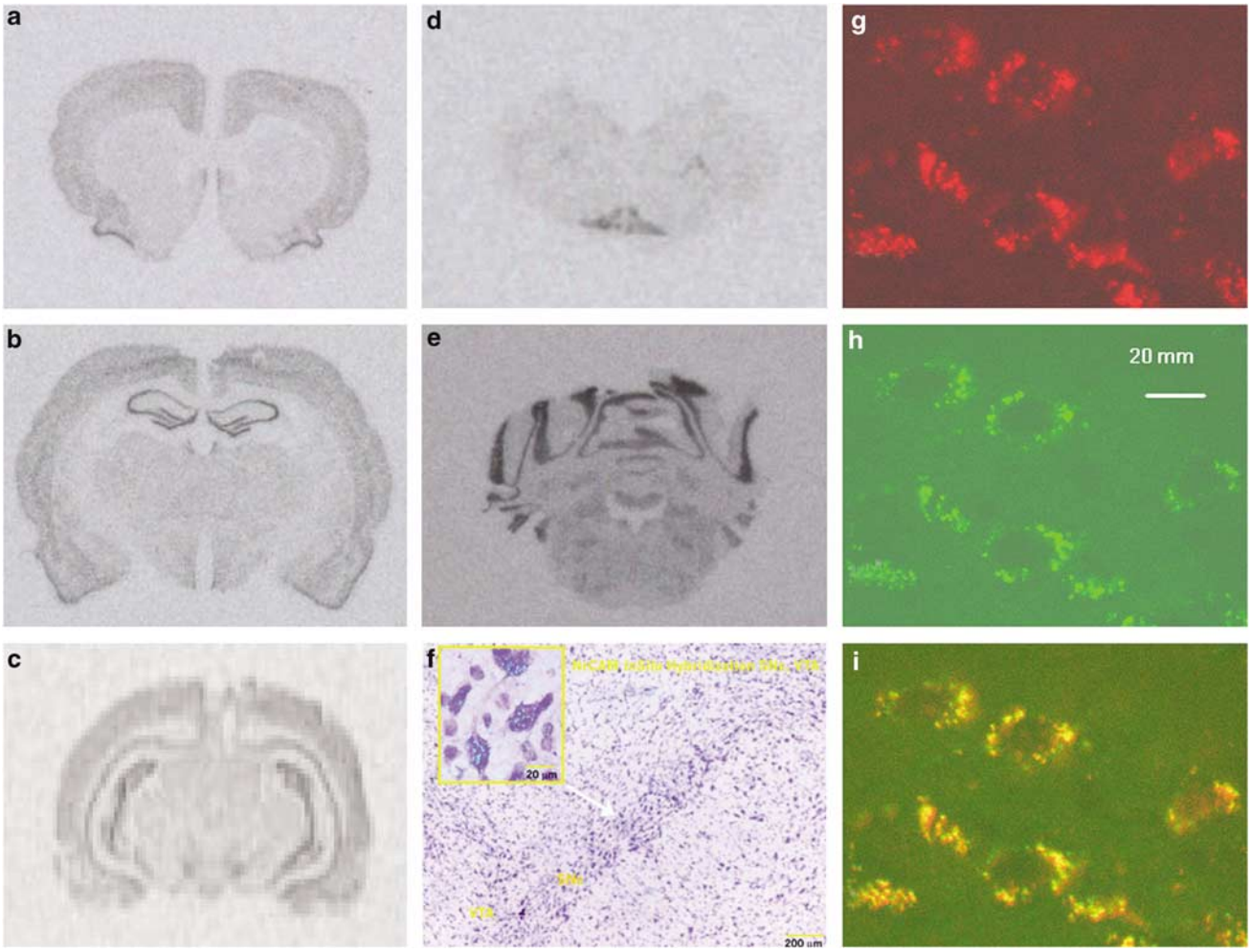

Figure 3 *In situ* hybridization autoradiographic and immunohistochemical documentation of the distributions of *NrCAM* mRNA and protein in the brain. (a–f) Hybridization to radiolabeled antisense probes complementary to common regions of the *NrCAM* 3′ untranslated regions. Film autoradiograms of brain sections containing: (a) forebrain, (b) midthalamus, (c) midbrain, (d) brainstem, and (e) cerebellum. (f) Higher magnification view of *in situ* hybridization emulsion autoradiogram of a Nissl-stained midbrain section hybridized with the radiolabeled 3′-UTR *NrCAM* probe. (g) *NrCAM* immunohistochemistry in midbrain sections detected with Alexa Fluor 594 (red) in midbrain sections. (h) Immunohistochemistry in the same midbrain section detecting immunoreactivity for the dopamine transporter (DAT) using Alexa Fluor 488 (green) in midbrain sections. (i) Overlay of G and H documenting *NrCAM* expression in many dopaminergic neurons. In repeated experiments, most (80%), but not all, DAT immunopositive neurons display *NrCAM* staining and *visa versa*.

precursor gene (*LAMB4*), and laminin β1 (*LAMB1*) gene (Figure 4).

NrCAM Region Markers and Haplotypes

Elucidation and validation of SNPs. NCBI and Celera databases, sequence alignments, and *NrCAM* genomic and cDNA resequencing allowed identification of the *NrCAM* missense SNP rs6958498/hCV25644546 that produces an Ala520Pro coding variant. We also identified four additional common and one rare coding region SNPs, an SNP in *NrCAM*'s 5′ untranslated region sequences and two SNPs in its 3′ untranslated region sequences. We could not identify the previously reported missense SNP rs1043895/hCV8856898 in any of 200 European-Americans sampled (data not shown).

Definition of NrCAM *3′ and 5′ blocks of restricted haplotype diversity.* Identifying these SNP variants allowed us to define 3′ and 5′ blocks of restricted haplotype diversity in European-American individuals. The 3′ haplotype block includes the rs1269634/hCV2686185/Ala520Pro variant; rs401433/hCV2298076/Ala710Ala variant and rs439587/hCV2298025 variant that encodes 1343c>a in the 3′UTR, and displays moderate linkage disequilibrium (Supplementary materials and data not shown). The more 5′ block of restricted haplotype diversity includes SNPs rs3763462/hCV2631385, rs1859769/hCV11607927, and rs2284284/hCV2686200. Haplotypes involving these markers provided information about at least four additional 5′ *NrCAM* SNPs that lie in introns, four that lie in 5′ exons, and five that lie in 5′ flanking sequences.

In African-American samples, more complex patterns of linkage disequlibrium produce smaller and more complex haplotype blocks especially noted in the 3′ haplotype block (Supplementary materials and data not shown). A region of historically higher recombination thus separates the 3′ and 5′ haplotype blocks in both ethnic samples, while additional

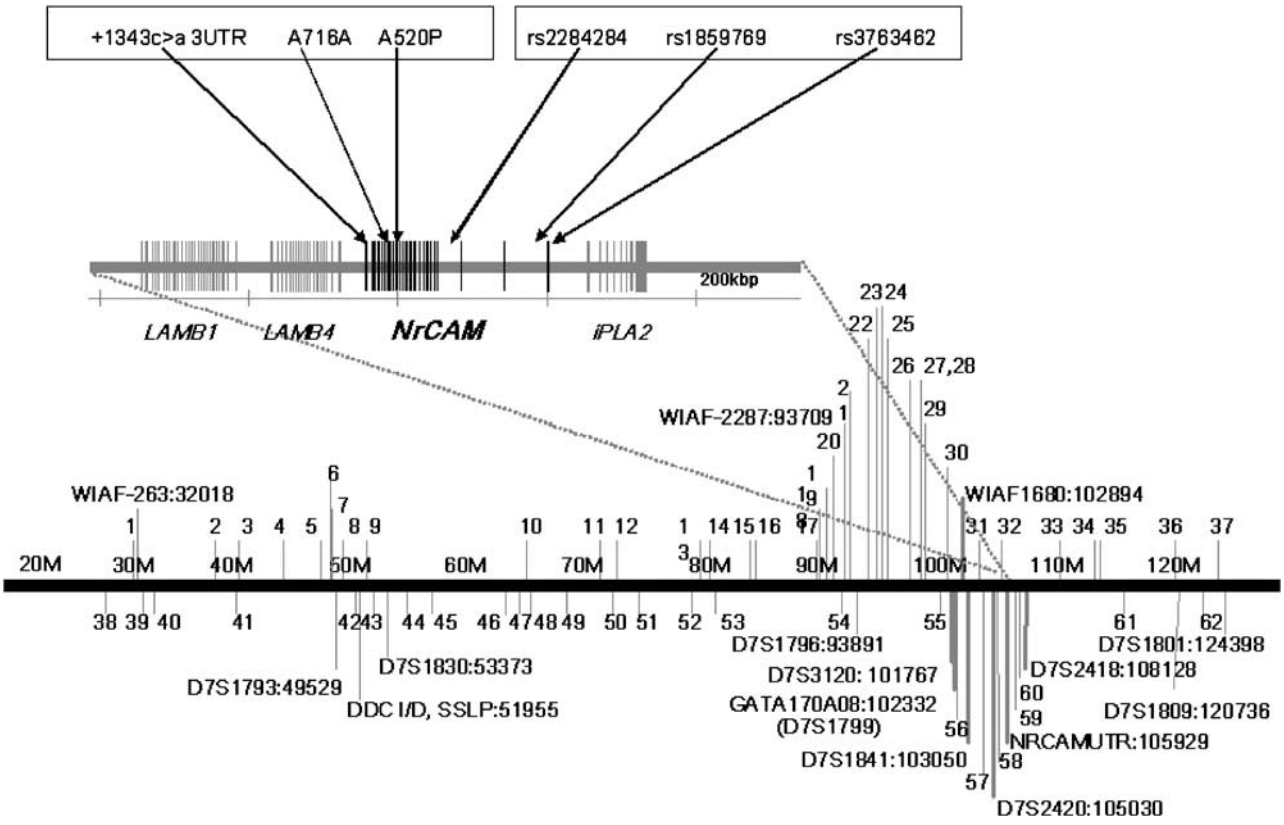

Figure 4 Diagram of the mid-chromosome 7 region subjected to initial hypothesis-generating and follow-up hypothesis-testing association studies. Positions of genes and markers are noted. Markers named here display nominally significant associations with addiction in either European- or African-American samples from NIDA. Other markers studied include: (1) WIAF-514, (2) WIAF-678, (3) WIAF-902, (4) WIAF-2308, (5) WIAF-1810, (6) WIAF-2750, (7) WIAF-2752, (8) WIAF-4576, (9) WIAF-1960, (10) WIAF-2601, (11) WIAF-3321, (12) WIAF-350, (13) WIAF-806, (14) WIAF-961, (15) WIAF-4581, (16) WIAF-4573, (17) WIAF-4537, (18) WIAF-4521, (19) WIAF-1772, (20) WIAF-3603, (21) WIAF-2264, (22) WIAF-550, (23) WIAF-570, (24) WIAF-1781, (25) WIAF-1477, (26) WIAF-3755, (27) WIAF-672, (28) WIAF-671, (29) WIAF-2086, (30) WIAF-807, (31) WIAF-983, (32) WIAF-2152, (33) WIAF-3292, (34) WIAF-3585, (35) WIAF-3285, (36) WIAF-3650, (37) WIAF-3309, (38) D7S2213, (40) UT6195, (41) D7S817, (42) D7S1818, (43) SSLP in *AC004920*, (44) SSLP in *AC006971*, (45) GGAT3D12, (46) D7S2472, 47: SSLP in *AC006001*, (48) D7S1839, (49) GTAT1A10, (50) UT6234, 51: GATA8G02, (52) GATA21D08, (53) D7S820, (54) D7S821, (55) ATA21D06, (56) D7S530, (57) D7S501, (58) D7S2459, (59) UT899, (60) D7S1817, (61) D7S2847, and (62) D7S2203. Enlargement shows the region subjected to follow-up studies including *NrCAM* and surrounding genes, with the positions of key markers that help to define the 5′ (left) and 3′ (right) *NrCAM* haplotypes indicated.

recombinations also appear to provide small haplotype blocks most notable in 3′ *NrCAM* aspects in African-American samples (data not shown). These patterns are generally in accord with those documented more recently in HapMap data (Supplementary material).

NrCAM Markers and Haplotype Associations with Substance Abuse Vulnerabilities

Testing the hypothesis that variants contained in 3′ NrCAM *haplotypes contribute to individual differences in human addiction vulnerability: identification of associations with opposite phases in European- and African-American samples.* To test this hypothesis, we first sought association between addiction and allelic frequencies at markers in *NrCAM*'s 3′ block of restricted haplotype diversity. The 3′ haplotype formed by rs6958498/hCV25644546/Ala520Pro, rs401433/hCV2298076/Ala710Ala, and rs439587/hCV2298025/3′UTR + 1343c > a was about twice as abundant in NIDA European-American controls as in abusers (nominal $p = 0.0006$) (Table 1). To seek generalization and extension of these initial results, we studied unrelated European-American individuals selected from COGA pedigrees. The 520Pro/Ala710c/ + 1343a 3′UTR haplotype was again more frequent in individuals who did not meet any alcoholism diagnosis by DSM criteria than in individuals with alcohol dependence ($p = 0.003$). To further test whether the 3′ 520Pro/Ala710c/ + 1343a 3′UTR haplotype was also present in different frequencies in addicts and controls, we tested NIDA African-American drug abusers *vs* controls. These individuals again displayed significant differences between 520Pro/Ala710c/ + 1343a 3′UTR haplotype frequencies in abusers and controls (nominal $p = 0.0006$). However, these samples displayed the opposite phase of association from that displayed by the two European-American samples. Frequencies of the addiction-associated 3′ *NrCAM* haplotype were thus higher in African-American abusers than in controls but lower in two samples of European-American substance abusers than in the corresponding control samples (Table 1).

Testing the hypothesis that variants contained in 5′ NrCAM *haplotypes contribute to individual differences in human addiction vulnerability: identification of*

associations with the same phase in European-American, African-American and Japanese samples. Since the phase of addiction vulnerability association of the 3′ *NrCAM* 520Pro/Ala710c/ + 1343a 3′UTR haplotype was similar in two European-American substance abuser/control comparisons but opposite in African-American samples (Table 1), we then asked whether more 5′ haplotypes might display association with the same phase in individuals of both ethnicities.

The *NrCAM* 5′ flanking region haplotype that includes rs3763462/hCV2631385, rs1859769/hCV11607927, and rs2284284/hCV2686200 displays significant differences between abusers and controls in each of the three samples tested. Further, this haplotype's association displays the same phase in comparisons of NIDA European-American polysubstance abusers *vs* controls ($p = 0.0002$), NIDA African-American polysubstance abusers *vs* controls ($p = 0.02$), and COGA European-American alcoholics *vs* controls ($p = 0.06$; Table 2). We were able to replicate the same finding in another addiction vulnerability sample of different ethnicity: in samples of Japanese alcoholics *vs* controls ($p = 0.01$). These cumulative positive data strongly support our hypothesis that *NrCAM* variants contribute to human interindividual differences in addiction vulnerability.

Contrasting results for markers at nearby genes. These positive data for *NrCAM* contrast with results obtained at nearby genes. Neither *LAMB1* missense hcv2193705/Arg1022Gln, *LAMB1* rs7561/hcv8856543/3′ untranslated region + 30C > A, *LAMB4* missense SNP rs1627354/hCV8856678/His1417Tyr, nor *LAMB4* intron SNP rs2286251/hCV16179224 display allelic frequency differences between abusers and controls (data not shown). Studies of four common exonic and five 5′ flanking region or intronic *iPLA2* variations reveal that none of these markers produces associations that displayed the same phase in comparisons of abuser *vs* control groups of European- and African-American samples, although several of the markers display nominally significant associations with addiction vulnerability in single samples (data not shown).

Table 1 Frequencies of 3′ *NrCAM* Haplotypes Formed by A520P, 716A g > c, and +1343a > c 3′UTR in Substance Abusing and Control Samples

	COGA cont. (112)	COGA abu. (65)	NIDA E.Am cont. (253)	NIDA E.Am abu. (366)	NIDA Af.Am cont. (98)	NIDA Af.Am abu. (226)
Aga	0.0100	0.0392	0.0343	0.0438	0.1054	0.1749
Agc	0.0546	0.0279	0.0647	0.0581	0.1370	0.0949
Aca	0.0051	0.0088	0.0293	0.0254	0.0660	0.0900
Acc	0.7338	0.7472	0.6049	0.6596	0.2223	0.1711
Pca	**0.1023****	**0.0265****	**0.0993*****	**0.0497*****	**0.0392****	**0.0990****
Pcc	0.0384	0.0525	0.0705	0.0561	0.1929	0.2087
Pga	0.0254	0.0178	0.0308	0.0341	0.1313	0.0742
Pgc	0.0303	0.0801	0.0662	0.0733	0.1060	0.0872

Global *p*-values calculated in each population are $p < 0.05$.
Pca haplotype frequency comparisons between abusers and controls are shown in bold.
**$p < 0.01$, ***$p < 0.001$.

Table 2 Frequencies of 5′ *NrCAM* Haplotypes Formed by rs3763462/hCV2631385, rs1859769/hCV1160727, and rs2284284/hCV2686200 in Substance Abusing and Control Samples

	COGA control (112)	COGA abusers (65)	NIDA E.Am cont. (170)	NIDA Eu.Am abu. (322)	NIDA Af.Am cont. (93)
AAA	0.0787	0.0691	0.0467	0.0396	0.0651
AAB	**0.3141**$^{+}$	**0.2304**$^{+}$	**0.3291*****	**0.2242*****	**0.1551***
ABA	0.0000	0.0000	0.0078	0.0258	0.0217
ABB	0.0090	0.0466	0.0193	0.0675	0.0000
BAA	0.0045	0.0082	0.0004	0.0423	0.0055
BAB	0.0000	0.0000	0.0238	0.0495	0.0000
BBA	0.2784	0.2920	0.2157	0.2199	0.4615
BBB	0.3153	0.3537	0.3572	0.3312	0.2911

Global *p*-values calculated in each population are COGA $p = 0.08$, NIDA Eur $p < 0.0001$, NIDA Af. $p = 0.01$.
The AAB haplotype frequency was compared between abusers and controls in each population, shown in bold.
$^{+}p = 0.06$, *$p < 0.05$, ***$p < 0.001$.

Haplotype-Specific Expression of *NrCAM* mRNA in Human Brain

NrCAM *haplotype association with reduced mRNA expression.* We hypothesized that functional *NrCAM* haplotypes might produce their effects on human addiction vulnerability, at least in part, by conferring different levels of *NrCAM* expression and/or regulation in ways that might contribute to individual differences in *NrCAM* mRNA levels in post-mortem human brains. To seek possible functional significance of the *NrCAM* locus haplotypes, we identified cerebral cortical, hippocampal, and midbrain samples from European-American individuals who were heterozygous for SNPs in *NrCAM* exons. We examined the ratios between the mRNAs marked by one allele, as defined using individual SNPs, *vs* the mRNAs marked by the other allele. These expression studies of allelic variants at eight SNPs within *NrCAM* revealed expression patterns skewed toward lower expression of one allele than the other (Figure 5a). The maximal differences in haplotype-specific mRNA expression correspond to the 'gcgccPcg' haplotype that is marked by the alleles: rs1269634/hCV2686185 = g, rs2072546/hCV2686182/N121N = c, rs1269621/hCV2686158/N319N = g, rs381318/hCV2298103/N404N = c, rs404287/hcv2298094/A509A = c, rs6958498/hCV25644546/A520P = P, rs401433/hCV2298076/A710A = c, and rs449077/hCV2298026/ + 666 3′UTR = g.

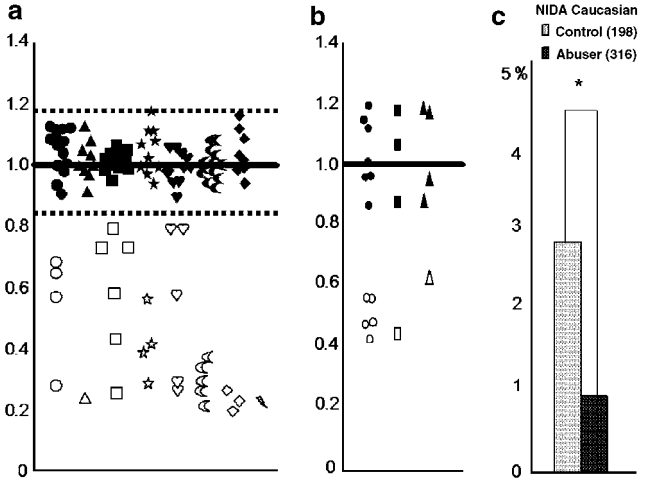

Figure 5 *NrCAM* mRNA expression levels, markers, and polysubstance abuse vulnerability. (a) Skew distribution of allele-specific *NrCAM* mRNA expression in brains from heterozygous European-American individuals. Ratios of expression levels for *NrCAM* mRNAs containing alternative alleles for eight exonic *NrCAM* SNPs are shown with circles = rs1269634 *(5UTR)* g/a, triangles = rs2072546 *(N121N)* c/t, squares = rs1269621 *(N319N)* g/a, stars = rs381318 *(V404V)* c/a, hearts = rs40428 *(A509A)* c/t, quarter moons = rs6958498 *(A520P)* P/A, diamonds = rs6958498 *(A710A)* c/g, lightning bolts = rs449077 *(3utr)* g/a. Subjects with nearly equal levels of expression of mRNAs corresponding to both allelic variants are indicated in black, and those with >2 standard deviations lower expression of one variant than the other indicated in open symbols. The heterozygote gcgccPcg haplotype that correlated with the reduced levels of expression was constructed from the allelic variants that displayed skewed distributions toward lower levels of expression. (b) *NrCAM* mRNA expression in cerebral cortical (circle), midbrain (square), and hippocampal (triangle) samples from individuals heterozygous for the gcgccPcg haplotype (white, open symbols) and individuals who lack the gcgccPcg haplotype (black, filled symbols). (c) Frequencies of the gcgccPcg *NrCAM* haplotype in European-American NIDA controls ($n = 198$; lighter bar) and abusers ($n = 316$; darker bar). *$p < 0.003$.

Comparisons of haplotype-specific NrCAM *mRNA expression levels in brains of heterozygous individuals.* mRNA corresponding to the gcgccPcg haplotype is expressed at an average of 26% of the levels of expression of mRNAs encoded by the alternative haplotypes in these samples from heterozygous individuals (Figure 5a).

Comparisons between levels of NrCAM *mRNA expression in brains of heterozygous individuals* vs *those with other hapoltypes.* Supporting results were obtained when we compared *NrCAM* mRNA levels in cerebral cortex, midbrain, and hippocampal samples from individuals who were heterozygotes for the gcgccPcg haplotype to samples from individuals who lacked a gcgccPcg haplotype (Figure 5b). Expression is about 40% lower in the brains of individuals who displayed a gcgccPcg haplotype. Much of this difference can be captured by a core two-SNP 'Pc' haplotype (data not shown).

Contrasting results for expression of nearby genes. Data for *NrCAM* allele specific expression contrast with the results of attempts to identify possible patterns of haplotype-specific differential expression of adjacent genes. None of these genes revealed evidence for haplotype-specific differential expression. iPLA2 expression from each haplotype was similar in heterozygotes for the rs42200/hCV2631461 5′UTR and novel 3′UTR SNPs. There were no allele-specific differences in expression of the hypothetical gene hCG2014062 (data not shown).

Association Studies Using the Differentially Expressed *NrCAM* Haplotype

Definition of the European-American gcgccPcg haplotype that is associated with differential levels of expression of *NrCAM* mRNA and the core Pc haplotype allowed us to seek associations between these differentially expressed haplotypes and substance abuse. The extended gcgccPcg SNP haplotype displays significant frequency differences between NIDA European-American controls and polysubstance abusers ($p \leqslant 0.01$) (Figure 5c). The core Pc haplotype based on rs6958498/hCV25644546/A526P P and rs401433/hCV2298076/A716A c displays significant associations in the NIDA European-American ($p = 0.0003$), NIDA African-American ($p = 0.02$), and COGA European-American ($p = 0.05$) samples (data not shown).

Reduced Morphine and Stimulant Reward in Heterozygous and Homozygous *NrCAM* Knockout Mice

We hypothesized that if individual differences in levels of *NrCAM* expression contributed to individual differences in addiction vulnerability in humans, then mice with altered levels of *NrCAM* expression might display differences in murine models of substance reward and dependence. Conditioned place preference provides a relatively robust test for alterations in the reward and reward-memories induced by abused substances and displays good correla-

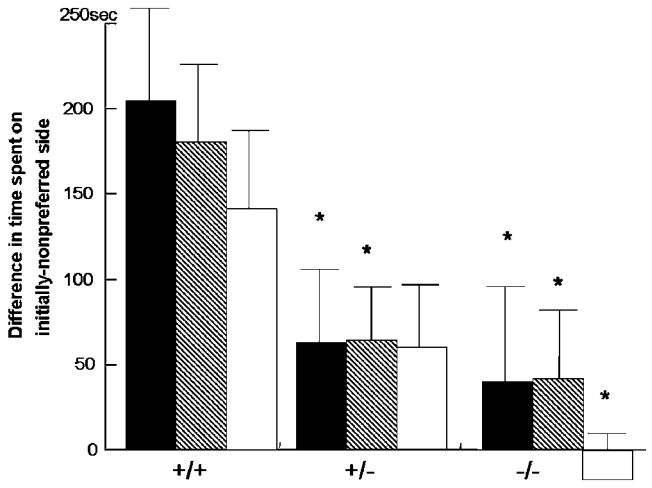

Figure 6 Morphine (black bars), cocaine (striped bars), and amphetamine (white bars)-conditioned place preferences in wild type (+/+), heterozygous (+/−), and homozygous (−/−) *NrCAM* knockout mice. Postexposure−pre exposure differences in the time spent on the previously drug paired side of the apparatus are noted in seconds. Morphine (20 mg/kg/ip) cocaine (20 mg/kg/s.c.) and amphetamine (2.0 mg/kg/i.p.) both cause wild-type mice to spend more time on the side paired with drug than they did prior to drug pairings. Morphine data derive from19 wild type, 31 heterozygous, and 16 homozygous *NrCAM* knockout mice, cocaine data from 17 wild type, 36 heterozygous, and 22 homozygous *NrCAM* knockout mice, and amphetamine data from nine wild type, 25 heterozygous, and 5 homozygous *NrCAM* knockout mice. Both heterozygous and homozygous *NrCAM* knockouts reduce this measure of morphine and cocaine reward, while results were significant for amphetamine only in homoaygotes One-way ANOVA $p<0.05$. **Post hoc* test: $p<0.05$ compared with wild-type mice.

tions with human addiction liabilities for many classes of abused substances. Heterozygous *NrCAM* knockout mice display 50–60% of the *NrCAM* expression of wild-type mice (data not shown), while homozygous knockouts display no *NrCAM* mRNA. Further, *NrCAM* knockout mice fail to display any robust deficit in mnemonic processes or locomotor abilities that would, *a priori,* invalidate conditioned place preference testing (MG and others, data not shown).

Both heterozygous and homozygous *NrCAM* knockout mice display striking reductions in their preferences for the places where they received 20 mg/kg morphine in comparison to wild-type control mice (Figure 6). Place preferences conditioned by 20 mg/kg of cocaine were also reduced in both heterozygous and homozygous *NrCAM* knockouts (Figure 6). The place preference conditioned by 2 mg/kg amphetamine was also attenuated, although only in homozygotes (Figure 6). There was no evidence for sedation found in locomotor data obtained from these mice during conditioning trials. Mice of all genotypes displayed similar sensitivities to the acute locomotor stimulant properties of all three drugs during conditioning trials (data not shown).

DISCUSSION

The present report documents convergent results from searches for drug-regulated genes and from association-based genome scans for drug abuse vulnerability alleles in a chromosome 7 region implicated in prior linkage studies. These data are supported by results of work on the *NrCAM* gene, its haplotypes, the brain distribution of *NrCAM*, the apparent impact of *NrCAM* haplotypes on levels of brain expression, and the impact of *NrCAM* deletion on drug reward in mouse models. Each of these approaches suggests that *NrCAM* could play important roles in neuronal connections and functions important for drug reward and drug addiction. Taken together, the data provide strong support for the idea that *NrCAM* haplotypes contribute to human individual differences in addiction vulnerability.

Subtractive hybridization/differential display, microarray, and related approaches have proven to be powerful tools, identifying hundreds of novel and known genes that are regulated after acute or chronic treatments with abused substances (Douglas *et al*, 1995; Schafer *et al*, 2001; Toyooka *et al*, 2002; Savoie *et al*, 2003; Sokolov *et al*, 2003; Wang *et al*, 1997). One of these genes is *NrCAM*, a single transmembrane domain protein member of a family of 'cell adhesion molecule' genes. The products of these 'cell adhesion molecule' genes can form homomeric or heteromeric recognition complexes that are important for normal brain development and for many of the ways in which adult brains alter functional connections.

The substantial levels of expression of *NrCAM* protein found in adult brain, its localization in specific neuronal populations, observations of substantial synaptic plasticity in circuits that express *NrCAM*, the likelihood that *NrCAM* function is regulated by phosphorylation (Grumet, 1997), and the likelihood that *NrCAM* can regulate important phosphorylation cascades (Schaefer *et al*, 1999; Kolkova *et al*, 2000) each make this cell adhesion molecule a strong candidate to influence cellular regulatory pathways important for short- and long-term actions of abused substances.

NrCAM *haplotypes, their expression and association with drug abuse vulnerability*. We have identified *NrCAM* polymorphisms, 3′ haplotypes, and 5′ haplotypes that are found at different frequencies in individuals without any significant lifetime use of any addictive substance when compared to individuals dependent on addictive substances. These haplotypes and the racial or ethnic differences in haplotyes and allele frequencies identified here are supported by recent HapMap data as well. The different phases of association for the 3′ *NrCAM* haplotype block that we have identified in different ethnic groups are consistent with the idea that this block is close to but does not contain the functionally important allelic variations. Finding that the association for the 5′ haplotype block is in the same phase in several ethnic groups is consistent with the idea that this block contains the key functional allelic variants. These observations are also in accord with observations that *NrCAM* haplotypes correlate with levels of *NrCAM* expression in post-mortem brain samples and that drugs regulate *NrCAM* expression. Variations in *NrCAM* regulation are thus the strongest candidate mechanisms to explain the effects of *NrCAM* haplotypes on addiction vulnerability.

None of these lines of evidence rules out the possibility that *NrCAM* variants that do not alter its regulated levels of

its expression could also contribute to addiction vulnerability, however. Alanine/proline missense substitutions in extracellular motifs might alter *NrCAM*'s binding properties. The rich patterns of differential splicing and exon use within the 3′ *NrCAM* haplotype block that we have identified might add to the diversity of *NrCAM* binding domains and allow *NrCAM* variants in these regions to subtly modify the cell-type specific recognition information that they appear to confer, while each of these polymorphisms did not always show association.

Reduced drug reward in NrCAM *knockout mice.* Haplotypes that correlate with reduced *NrCAM* expression in human post-mortem brains are found less frequently in human substance abusers than in human controls. These lines of evidence provide strong correlates with data obtained from heterozygous knockout mice. Mice with reduced levels of *NrCAM* expression manifest less preference for the places associated with injections of morphine or cocaine. Mice with no *NrCAM* expression demonstrate mutually no conditioned place preferences for morphine, cocaine, or amphetamine. These striking and convergent results should be considered in the context of possible confounding influences. It is conceivable that some of the effects observed in these single-dose CPP studies could be due to left- or rightward shifts in the dose–effect relationships of these drugs. While more detailed dose–effect studies will be necessary to identify such effects, it seems that potency shifts alone would be highly unlikely to confer the convergent results obtained here. Conceivably, alterations in drugs' sedative or stimulant properties might contribute to the CPP results obtained here. However, locomotor data obtained during conditioning sessions provide no support for such effects. We cannot totally exclude modest contributions of *NrCAM* knockout effects on general memory systems in the observations made here. However, there is a lack of large effects of *NrCAM* knockout on most memory tests that has been observed in preliminary studies of these animals (Grumet and Matzel unpublished observations), with only very modest influences in heterozygotes. The contrasting large, and consistent effects of *NrCAM* knockouts on morphine-, amphetamine-, and cocaine-conditioned place preferences suggests that most of the altered drug effects identified in these assays are unlikely to come from mnemonic effects alone.

Contribution of NrCAM *variation to COGAwave I chromosome 7 linkage peak.* The current data provide support for association-based genome scanning and point to its ability to identify specific vulnerability-associated genes and haplotypes. Our identification of *NrCAM* haplotype associations in COGA samples is consistent with contributions of the identified haplotype to the linkage signal reported by Reich *et al* in 1997. However, *NrCAM* variants appear unlikely to confer all of these linkage signals. Modest association signals found in other parts of this broad chromosome 7 region (HI and GRU, unpublished observations, 2004) could be consistent with contributions of variants at other loci that fall under the relatively large chromosome 7 linkage peak to the observed COGA Wave I linkage results. It is also interesting to note that the large linkage signals identified in this region in COGA Wave I samples do not appear as intensely in studies of smoking and alcohol phenotypes in COGA Wave II samples (Bierut *et al*, 2004). While there is no generally agreed way to estimate the power of association genome scanning approaches, further studies in additional and population-based samples will help to accurately estimate the addiction risks attributable to *NrCAM* haplotypes and other gene variants that lie in mid-chromosome 7.

Roles of neuronal cell adhesion molecule variants in addiction and other brain disorders. The current data are in accord with observations from recently reported studies of autism that describe contributions of 5′ *NrCAM* haplotypes to autism (Bonora *et al*, 2005). These additional observations support the idea that variants found in 5′ *NrCAM* haplotypes exert functional impact on the gene and its expression. *NrCAM* haplotypes thus appear likely to provide plieotrophic contributions to brain and behavior and contributions to vulnerability to addiction and autism that are likely to depend on which other genetic and environmental influences are present.

Potential roles in multiple brain functions and brain disease states are supported by *in situ* hybridization and immunohistochemical results. These data document *NrCAM* expression in regions such as hippocampus that are important for mnemonic functions and in midbrain dopaminergic neurons important for reward. *NrCAM* could thus influence the establishment and maintenance of cellular regulatory pathways important for drug reward and drug memory circuits. Drug regulation of *NrCAM* expression in some of these brain regions provides other levels of complexity. *NrCAM* expression, regulation, and individual differences are thus all well-positioned to play roles in responses to addictive drugs and in the development of addictions.

NrCAM is unlikely to play such roles alone, however. *NrCAM* is a member of a family of genes that can form homophilic or heterophilic recognition complexes that are important for normal brain development and can play key roles in adult brain connectivities. Data from higher density genome scanning SNP arrays and assessments of genes for other family members both suggest that human individual differences in other cell adhesion molecule genes could contribute to addiction vulnerability (Q-R Liu, GRU *et al*, in preparation; HI and GRU, in preparation). Molecules with Ig/fibronectin/single transmembrane domain/tyrosine kinase motifs such as those displayed by *NrCAM*, molecules with EGF-like motif/single transmembrane domain/tyrosine kinase motifs, and nontransmembrane cell adhesion molecules that contain glycoprotein membrane anchors are each implicated by these studies and/or by studies that document regulation by abused substances (Grigorenko *et al*, 2002; Miller and Luo, 2002; Dunckley and Lukas, 2003) (HI and GRU, in preparation). Regulatory events that involve *NrCAM* and other cell adhesion molecules appear to play significant roles in adaptive process that follow drug administration, including those relevant for addiction.

Convergence between positional cloning and disease-regulated gene results. The current observations concerning *NrCAM* appear to represent a striking example of

convergence between genome scanning and gene expression results for addiction, a phenomenon that has been termed convergent functional genomics in studies of depression (Niculescu and Kelsoe, 2001). Gene expression data helped to focus our attention on an appropriate locus in genome scanning efforts. Regulatory differences are likely to contribute to the effects of many functional human allelic variants. Disease-regulated genes located on chromosomal regions in which markers are linked to or associated with the same disease should be considered strong pathogenic candidates and examined with care in fine mapping studies. As better and better validated animal models for disease expression studies and improved human gene expression profiles are available for more and more disorders, we anticipate more examples of the power of this approach.

ACKNOWLEDGEMENTS

We acknowledge financial support from NIDA-IRP, NIH/DHSS. This work was supported from the Ministry of Education, Culture, Sports, Science and Technology of Japan aided collection of Japanese samples. Human brain tissues were obtained from Brain and Tissue Bank for Developmental Disorders (B&T Bank) supported through NIH contract NO1-HD-1-3138. We are grateful for careful assistance with clinical data collection from Judith Hess, Fely Carillo and Brenda Campbell, assistance with initial microarray experiments from Zhicheng Lin and generous access to COGA samples supported by the NIAAA and the COGA investigators. Some of these data were generated through the use of the Celera Discovery System and Celera's associated database. GenBank Accession #: rNc1: AY574272; rNc14: AY574273; rNc3: AY574274; rNc6: AY574275; rNc7: AY574276; rNc17: AY574277; rNrCAM_short: AY528244; mNrCAM_short: AY528242; hNrCAM_short: AY528240.

REFERENCES

Bierut LJ, Rice JP, Goate A, Hinrichs AL, Saccone NL, Foroud T *et al* (2004). A genomic scan for habitual smoking in families of alcoholics: common and specific genetic factors in substance dependence. *Am J Med Genet A* **124**: 19–27.

Bonora E, Lamb JA, Barnby G, Sykes N, Moberly T, Beyer KS *et al* (2005). Mutation screening and association analysis of six candidate genes for autism on chromosome 7q. *Eur J Hum Genet* **13**: 198–207.

Douglas J, McKinzie AA, Couceyro P (1995). PCR differential display identifies a rat brain mRNA that is transcriptionally regulated by cocaine and amphetamine. *J Neurosci* **15**: 2471–2481.

Dunckley T, Lukas RJ (2003). Nicotine modulates the expression of a diverse set of genes in the neuronal SH-SY5Y cell line. *J Biol Chem* **278**: 15633–15640.

Grigorenko E, Kittler J, Clayton C, Wallace D, Zhuang S, Bridges D *et al* (2002). Assessment of cannabinoid induced gene changes: tolerance and neuroprotection. *Chem Phys Lipids* **121**: 257–266.

Grumet M (1997). Nr-CAM: a cell adhesion molecule with ligand and receptor functions. *Cell Tissue Res* **290**: 423–428.

Gynther LM, Carey G, Gottesman II, Vogler GP (1995). A twin study of non-alcohol substance abuse. *Psychiatry Res* **56**: 213–220.

Hall FS, Goeb M, Li XF, Sora I, Uhl GR (2004). μ-opioid receptor knockout mice display reduced cocaine conditioned place preference but enhanced sensitization of cocaine-induced locomotion. *Mol Brain Res* **121**: 123–130.

Ishiguro H, Arinami T, Saito T, Akazawa S, Enomoto M, Mitushio H *et al* (1998). Association study between the −141C Ins/Del and TaqI A polymorphisms of the dopamine D2 receptor gene and alcoholism. *Alcohol Clin Exp Res* **22**: 845–848.

Karkowski LM, Prescott CA, Kendler KS, Neale MC (2000). Multivariate assessment of factors influencing illicit substance use in twins from female–female pairs. *Am J Med Genet* **96**: 665–670.

Kendler KS, Karkowski LM, Neale MC, Prescott CA (2000). Illicit psychoactive substance use, heavy use, abuse, and dependence in a US population-based sample of male twins. *Arch Gen Psychiatry* **57**: 261–269.

Kendler KS, Karkowski LM, Prescott CA (1999). The assessment of dependence in the study of stressful life events: validation using a twin design. *Psychol Med* **29**: 1455–1460.

Kendler KS, Neale MC, Heath AC, Kessler RC, Eaves LJ, Goodwin DW (1994). A twin-family study of alcoholism in women Familial alcoholism: a separate entity? *Am J Psychiatry* **151**: 707–715.

Kendler KS, Prescott CA (1998). Cannabis use, abuse, and dependence in a population-based sample of female twins. *Am J Psychiatry* **155**: 1016–1022.

Kolkova K, Novitskaya V, Pedersen N, Berezin V, Bock E (2000). Neural cell adhesion molecule-stimulated neurite outgrowth depends on activation of protein kinase C and the Ras-mitogen-activated protein kinase pathway. *J Neurosci* **20**: 2238–2246.

Liu QR, Lopez-Corcuera B, Mandiyan S, Nelson H, Nelson N (1993). Molecular characterization of four pharmacologically distinct gamma-aminobutyric acid transporters in mouse brain [corrected]. *J Biol Chem* **268**: 2106–2112.

Liu QR, Zhang PW, Zhen Q, Walther D, Wang XB, Uhl GR (2002). KEPI, a PKC-dependent protein phosphatase 1 inhibitor regulated by morphine. *J Biol Chem* **277**: 13312–13320.

Long JC, Knowler WC, Hanson RL, Robin RW, Urbanek M, Moore E *et al* (1998). Evidence for genetic linkage to alcohol dependence on chromosomes 4 and 11 from an autosome-wide scan in an American Indian population. *Am J Med Genet* **81**: 216–221.

McNaught KS, Belizaire R, Jenner P, Olanow CW, Isacson O (2002). Selective loss of 20S proteasome alpha-subunits in the substantia nigra pars compacta in Parkinson's disease. *Neurosci Lett* **326**: 155–158.

Merikangas KR, Swendsen JD, Preisig MA, Chazan RZ (1998). Psychopathology and temperament in parents and offspring: results of a family study. *J Affect Disord* **51**: 63–74.

Miller MW, Luo J (2002). Effects of ethanol and transforming growth factor beta (TGF beta) on neuronal proliferation and nCAM expression. *Alcohol Clin Exp Res* **26**: 1281–1285.

Morales M, Bloom FE (1997). The 5-HT3 receptor is present in different subpopulations of GABAergic neurons in the rat telencephalon. *J Neurosci* **17**: 3157–3167.

Moriwaki A, Wang JB, Svingos A, van Bockstaele E, Cheng P, Pickel V *et al* (1996). mu Opiate receptor immunoreactivity in rat central nervous system. *Neurochem Res* **21**: 1315–1331.

Niculescu III AB, Kelsoe JR (2001). Convergent functional genomics: application to bipolar disorder. *Ann Med* **33**: 263–271.

Persico AM, Bird G, Gabbay FH, Uhl GR (1996). D2 dopamine receptor gene TaqI A1 and B1 restriction fragment length polymorphisms: enhanced frequencies in psychostimulant-preferring polysubstance abusers. *Biol Psychiatry* **40**: 776–784.

Reich T (1996). A genomic survey of alcohol dependence and related phenotypes: results from the Collaborative Study on the Genetics of Alcoholism (COGA). *Alcohol Clin Exp Res* **20**: 133A–137A.

Reich T, Edenberg HJ, Goate A, Williams JT, Rice JP, Van Eerdewegh P *et al* (1998). Genome-wide search for genes

affecting the risk for alcohol dependence. *Am J Med Genet* **81**: 207–215.

Sakurai T, Lustig M, Nativ M, Hemperly JJ, Schlessinger J, Peles E *et al* (1997). Induction of neurite outgrowth through contactin and Nr-CAM by extracellular regions of glial receptor tyrosine phosphatase beta. *J Cell Biol* **136**: 907–918.

Savoie CJ, Aburatani S, Watanabe S, Eguchi Y, Muta S, Imoto S *et al* (2003). Use of gene networks from full genome microarray libraries to identify functionally relevant drug-affected genes and gene regulation cascades. *DNA Res* **10**: 19–25.

Schaefer AW, Kamiguchi H, Wong EV, Beach CM, Landreth G, Lemmon V (1999). Activation of the MAPK signal cascade by the neural cell adhesion molecule L1 requires L1 internalization. *J Biol Chem* **274**: 37965–37973.

Schafer GL, Crabbe JC, Wiren KM (2001). Ethanol-regulated gene expression of neuroendocrine specific protein in mice: brain region and genotype specificity. *Brain Res* **897**: 139–149.

Smith SS, O'Hara BF, Persico AM, Gorelick DA, Newlin DB, Vlahov D *et al* (1992). Genetic vulnerability to drug abuse. The D2 dopamine receptor Taq I B1 restriction fragment length polymorphism appears more frequently in polysubstance abusers. *Arch Gen Psychiatry* **49**: 723–727.

Sokolov BP, Polesskaya OO, Uhl GR (2003). Mouse brain gene expression changes after acute and chronic amphetamine. *J Neurochem* **84**: 244–252.

Sora I, Hall FS, Andrews AM, Itokawa M, Li XF, Wei HB *et al* (2001). Molecular mechanisms of cocaine reward: combined dopamine and serotonin transporter knockouts eliminate cocaine place preference. *Proc Natl Acad Sci USA* **98**: 5300–5305.

Stallings MC, Hewitt JK, Beresford T, Heath AC, Eaves LJ (1999). A twin study of drinking and smoking onset and latencies from first use to regular use. *Behav Genet* **29**: 409–421.

Toyooka K, Usui M, Washiyama K, Kumanishi T, Takahashi Y (2002). Gene expression profiles in the brain from phencyclidine-treated mouse by using DNA microarray. *Ann NY Acad Sci* **965**: 10–20.

True WR, Heath AC, Scherrer JF, Xian H, Lin N, Eisen SA *et al* (1999a). Interrelationship of genetic and environmental influences on conduct disorder and alcohol and marijuana dependence symptoms. *Am J Med Genet* **88**: 391–397.

True WR, Xian H, Scherrer JF, Madden PA, Bucholz KK, Heath AC *et al* (1999b). Common genetic vulnerability for nicotine and alcohol dependence in men. *Arch Gen Psychiatry* **56**: 655–661.

Tsuang MT, Lyons MJ, Eisen SA, Goldberg J, True W, Lin N *et al* (1996). Genetic influences on DSM-III-R drug abuse and dependence: a study of 3, 372 twin pairs. *Am J Med Genet* **67**: 473–477.

Tsuang MT, Lyons MJ, Harley RM, Xian H, Eisen S, Goldberg J *et al* (1999). Genetic and environmental influences on transitions in drug use. *Behav Genet* **29**: 473–479.

Tsuang MT, Lyons MJ, Meyer JM, Doyle T, Eisen SA, Goldberg J *et al* (1998). Co-occurrence of abuse of different drugs in men: the role of drug-specific and shared vulnerabilities. *Arch Gen Psychiatry* **55**: 967–972.

Uhl GR (1999). Molecular genetics of substance abuse vulnerability: a current approach. *Neuropsychopharmacology* **20**: 3–9.

Uhl GR (2004). Molecular genetics of substance abuse vulnerability: remarkable recent convergence of genome scan results. *Ann NY Acad Sci* **1025**: 1–13.

Uhl GR, Gold LH, Risch N (1997). Genetic analyses of complex behavioral disorders. *Proc Natl Acad Sci USA* **94**: 2785–2786.

Uhl GR, Kitayama S (1993). A cloned dopamine transporter. Potential insights into Parkinson's disease pathogenesis. *Adv Neurol* **60**: 321–324.

Uhl GR, Liu QR, Naiman D (2002). Substance abuse vulnerability loci: converging genome scanning data. *Trends Genet* **18**: 420–425.

Uhl GR, Liu QR, Walther D, Hess J, Naiman D (2001). Polysubstance abuse-vulnerability genes: genome scans for association, using 1,004 subjects and 1,494 single-nucleotide polymorphisms. *Am J Hum Genet* **69**: 1290–1300.

Wang B, Williams H, Du JS, Terrett J, Kenwrick S (1998). Alternative splicing of human NrCAM in neural and nonneural tissues. *Mol Cell Neurosci* **10**: 287–295.

Wang XB, Funada M, Imai Y, Revay RS, Ujike H, Vandenbergh DJ *et al* (1997). rGbeta1: a psychostimulant-regulated gene essential for establishing cocaine sensitization. *J Neurosci* **17**: 5993–6000.

Supplementary Information accompanies the paper on the Neuropsychopharmacology website (http://www.nature.com/npp).